Supporting Information

Impact of the metal center and functionalization on the mechanical behavior of the MIL-53 Metal Organic Frameworks

Pascal G. Yot,[*[a]] Ke Yang,[a] Vincent Guillerm,[b] Florence Ragon,[b] Vladimir Dmitriev,[c] Paraskevas Parisiades,[d] Erik Elkaïm,[e] Thomas Devic,[b] Patricia Horcajada,[b] Christian Serre,[b] Norbert Stock,[f] John P. S. Mowat,[g] Paul A. Wright,[g] Gérard Férey,[e] Guillaume Maurin,[a]

[a] Institut Charles Gerhardt Montpellier UMR 5253, CC15005, Université de Montpellier, Place Eugène Bataillon, F-34095 Montpellier cedex 05, France.

[b] Institut Lavoisier Versailles UMR 8180, Université de Versailles St-Quentin, 45, avenue des Etats-Unis, F-78035 Versailles cedex, France.

[c] Swiss Norvegian Beamlines, European Synchrotron Radiation Facility, F-3800 Grenoble, France.

[d] High Pressure Beamline (ID27), European Synchrotron Radiation Facility (BM01), F-3800 Grenoble, France.

[e] CRISTAL beamline, Synchrotron Soleil, L'orme des Merisiers, Saint-Aubin - BP 48, F-91192 Gif-sur-Yvette cedex, France.

[f] Institute für Anorganische Chemie,Christian-Albrechts-Universität, Max-EythStraße2, D 24118 Kiel, Germany.

[g] EaStCHEM School of Chemistry, University of St. Andrews, Purdie Building, North Haugh, St. Andrews, Fife KY16 9ST, United Kingdom.

1. Synchrotron powder X-ray diffraction

1.1. Experiments at the Swiss Norvegiam Beamline at ESRF

Diffraction patterns were collected using MAR345 image plate detector, a monochromatic beam with the wavelength of 0.694120 Å. Pressures were generated a DAC with flat culets of diameter 600 μm. The beam was slit collimated to 100x100 μm^2. The sample to-detector distance (350 mm) and parameters of the detector were calibrated using NIST standard LaB_6.

1.2. Experiments at the ID27 High Pressure Beamline at ESRF

High energy 2-D images were collected on a MARCCD 165 using a wavelength λ=0.37380 Å and the sample to detector distance (d=450.14 mm) was determined after calibration using NIST standard LaB_6. Beam size of 20x20 μm^2 was used during the experiment. Pressures were generated using Membrane Diamond Anvill Cells.

1.3. Experiments at the CRISTAL beamline at Synchrotron Soleil

All the two dimensional images collected by a RayoniX SX-165 CCD detector. Wavelength λ=0.5100 Å and sample to detector (d=302.56 mm) sample were determined using NIST standard LaB_6. The beam size used was $50\times50\,\mu m^2$ was selected by a pair of slits located 800 mm upstream the sample.

Two-dimensional diffraction images were integrated using FIT2D software [1]. Quasi-hydrostatic conditions were provide by Silicone oil (AP100, Fluka). Pressures were measured from the shift of the ruby R1 fluorescence line [2]. All diffraction measurements were performed increasing the pressure in the range 10^{-7}-3 GPa. The unit-cell parameters were determined by indexing the X-ray powder diffraction patterns, using DICVOL6 [3] followed by a Le Bail fit using Jana 2006 software [4].

Table S1. Unit cell parameters obtained for all the hydrated MIL-53(M)_X forms with M=Al, Cr, Sc and X=NO_2, Cl, CH_3.

Pressure	**S. G.**	**a (Å)**	**b (Å)**	**c (Å)**	**α (°)**	**β (°)**	**γ (°)**	**V (Å^3)**
MIL-53(Al)								
Atm.	*C2/c*	19.446(2)	7.599(2)	6.558(8)		104.17(1)		851.6(3)
1.36 GPa	*P-1*	6.554(3)	10.245(1)	13.136(3)	108.05(3)	90.77(3)	105.62(5)	804.5(2)
MIL-53(Al)_NO_2								
Atm.	*C2/c*	19.743(3)	8.243(8)	6.647(7)		106.71(1)		1036.7(1)
MIL-53(Cr)								
Atm.	*C2/c*	19.645(2)	7.627(5)	6.776(5)		104.37(1)		983.4(2)
0.51 GPa	*P-1*	6.775(2)	10.435(3)	13.204(3)	108.38(2)	92.81(3)	104.00(3)	939.6(2)
MIL-53(Cr)_Cl								
Atm.	*C2/c*	20.017(4)	7.883(8)	6.824(8)		106.67(2)		1031.5(4)
MIL-53(Cr)_CH_3								
Atm.	*C2/c*	20.062(2)	7.937(1)	6.820(1)		106.80(1)		1039.6(1)
MIL-53(Fe)								
Atm.	*C2/c*	19.758(4)	7.519(1)	6.831(1)		103.80(2)		985.3(3)
0.40 GPa	*P-1*	7.072(1)	10.844(1)	13.512(2)	110.52(1)	88.47(1)	103.31(1)	942.7(5)
MIL-53(Sc)								
Atm.	*P-1*	19.766(4)	7.609(2)	12.778(2)	88.27(2)	92.05(2)	91.46(2)	1917.5(2) *(958.6(2))*

1.4. MIL-53(Cr)

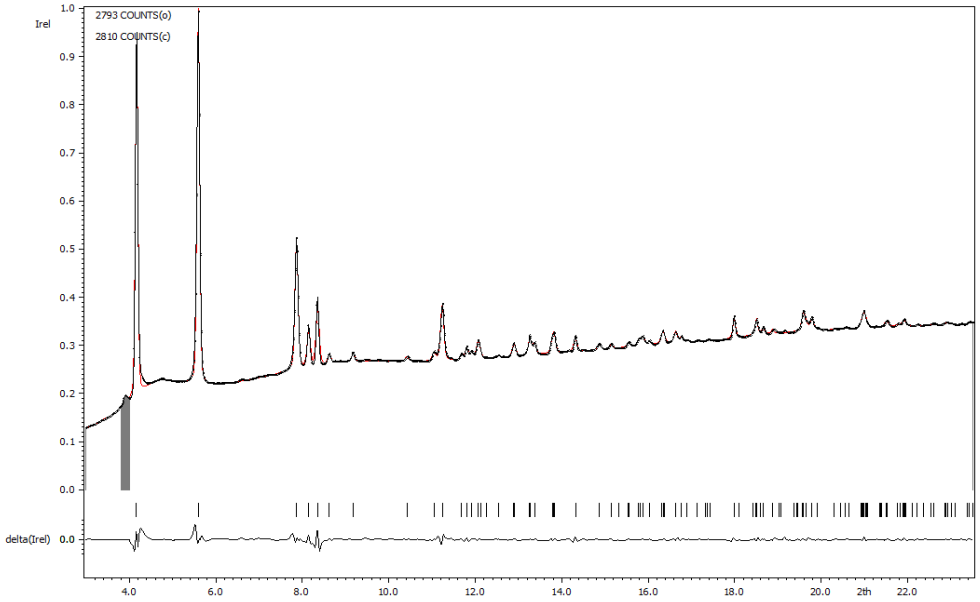

Figure S1. Structure-independent refinement of the unit-cell of the diffraction pattern obtained for the MIL-53(Cr), space group *C2/c* : a=19.645(2) Å, b=7.627(5) Å, c=6.776(5) Å, β=104.37(1)° V=983.4(2)Å^3 (Rp: 0.57, Rwp: 0.84, λ=0.69412 Å) at atmospheric pressure (first step of the experiment).

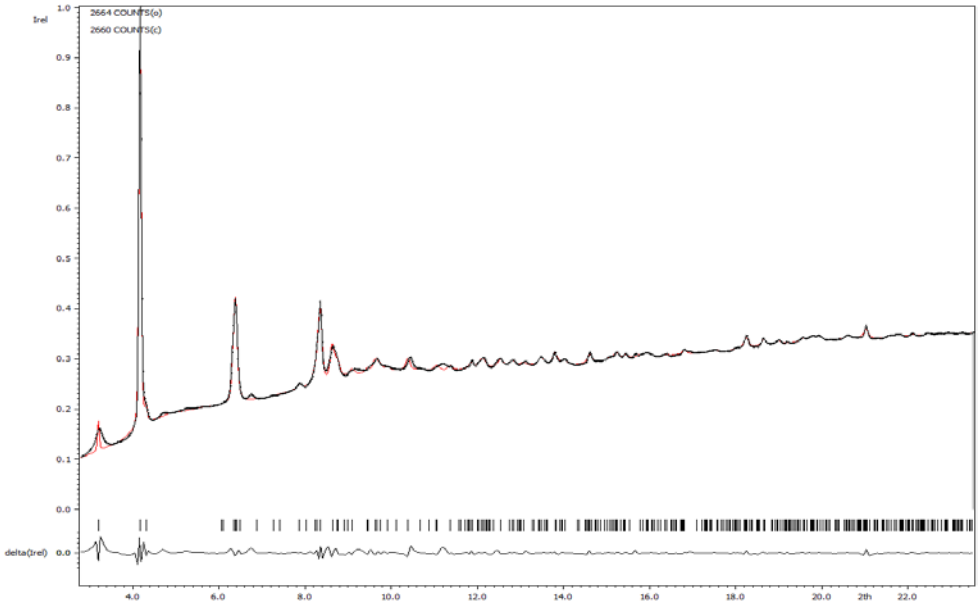

Figure S2. Structure-independent refinement of the unit-cell of the diffraction pattern obtained for the MIL-53(Cr), space group *P-1*: a=6.775(2) Å, b=10.435(3) Å, c=13.204(3) Å, α=108.38(2)°, β=92.81(3)°, γ=104.00(3)° V=939.6(2) Å^3 (Rp: 0.43, Rwp: 0.69, λ=0.69412 Å) at atmospheric pressure (first step of the experiment).

1.5. MIL-53(Al)

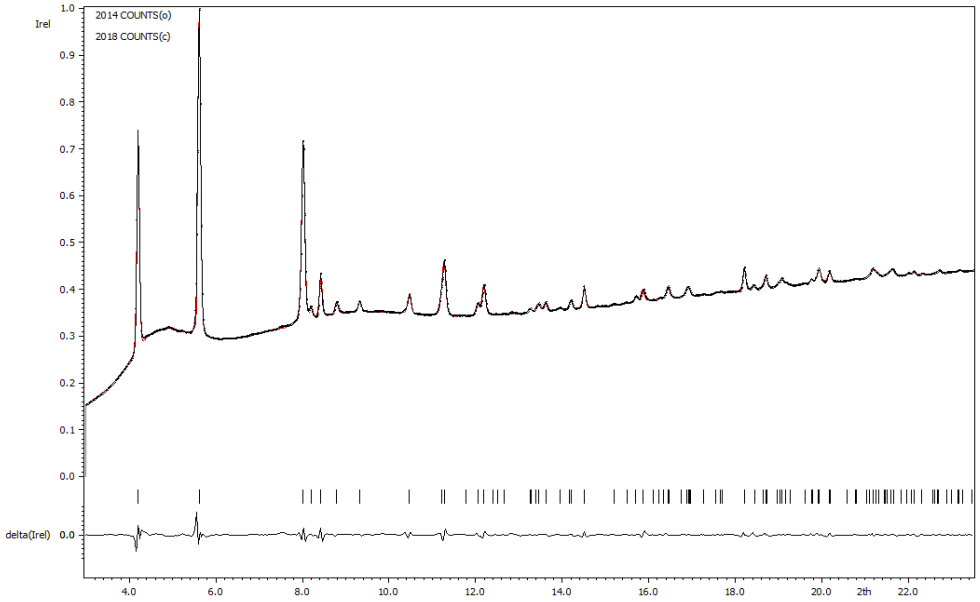

Figure S3. Structure-independent refinement of the unit-cell of the diffraction pattern obtained for the MIL-53(Al), space group *C2/c* : a=19.446(2) Å, b=7.599(6) Å, c=6.558(8) Å, β=104.17(1)° V=851.6(3) Å^3 (Rp: 0.74, Rwp: 0.99, λ=0.69412 Å) at atmospheric pressure (first step of the experiment).

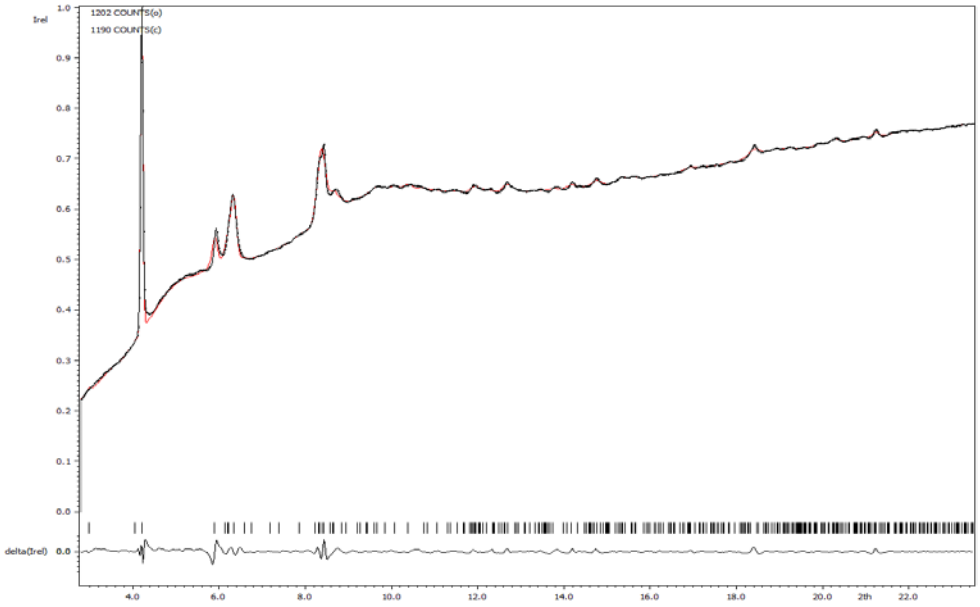

Figure S4. Structure-independent refinement of the unit-cell of the diffraction pattern obtained for the MIL-53(Al), space group *P-1* : a=6.554(3) Å, b=10.245(1) Å, c=13.136(3) Å, α=108.05(3)°, β=90.77(3)°, γ=105.62(5)° V=804.5(2) Å^3 (Rp: 0.32, Rwp: 1.50, λ=0.69412 Å) at atmospheric pressure (first step of the experiment).

1.6. MIL-53(Fe)

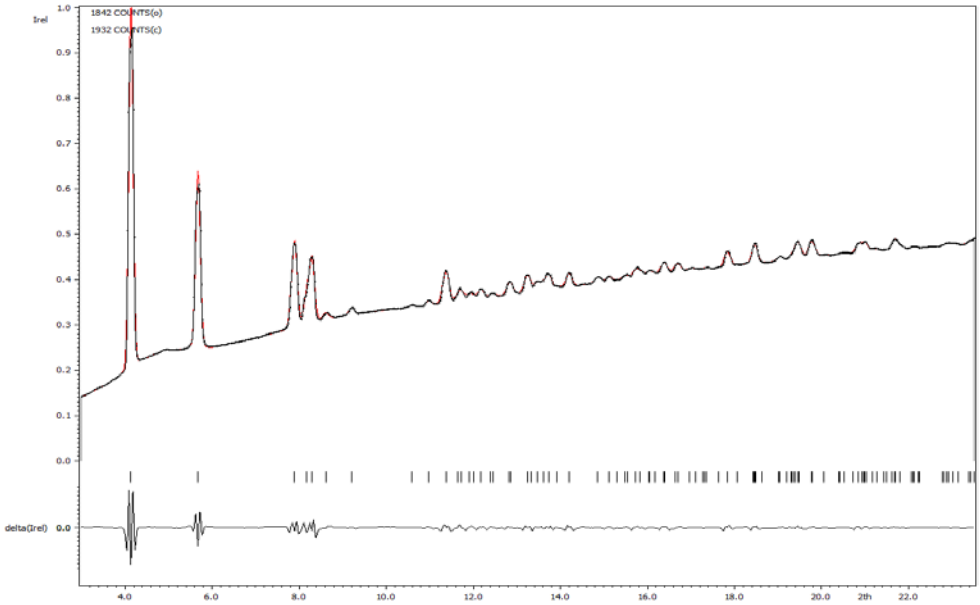

Figure S5. Structure-independent refinement of the unit-cell of the diffraction pattern obtained for the MIL-53(Fe), space group *C2/c* : a=19.758(4) Å, b=7.519(1) Å, c=6.831(1) Å, β=103.80(2)° V=985.3(3)Å^3 (Rp: 0.60, Rwp: 0.95, λ=0.69412 Å) at atmospheric pressure (first step of the experiment).

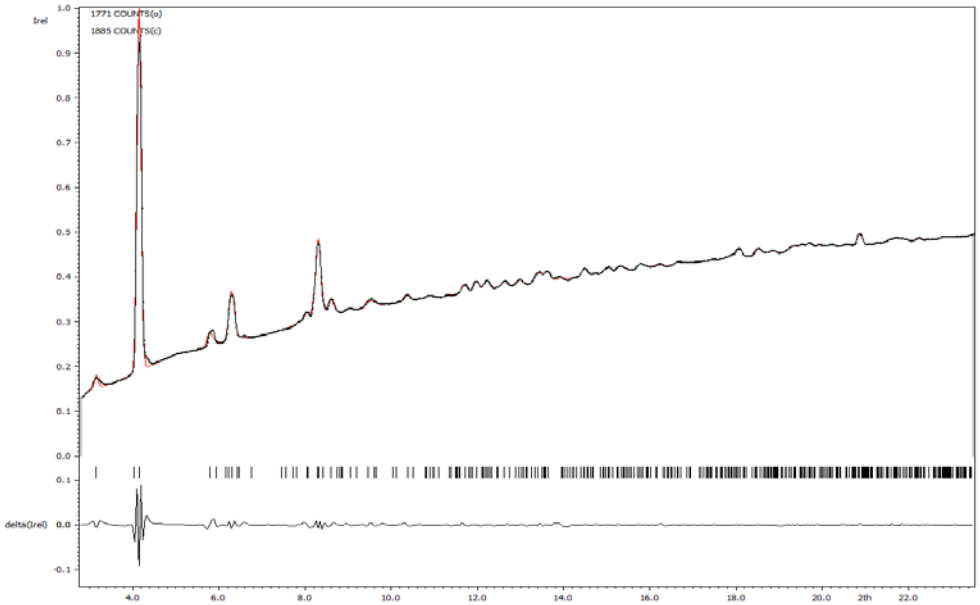

Figure S6. Structure-independent refinement of the unit-cell of the diffraction pattern obtained for the MIL-53(Fe), space group *P-1* : a=7.072(1) Å, b=10.844(1) Å, c=13.512(2) Å, α=110.52(1)°, β=88.47(1)°, γ=103.31(1) V=942.7(5)Å^3 (Rp: 0.46, Rwp: 0.78, λ=0.51000 Å) at atmospheric pressure (first step of the experiment).

1.7. MIL-53(Cr)_Cl

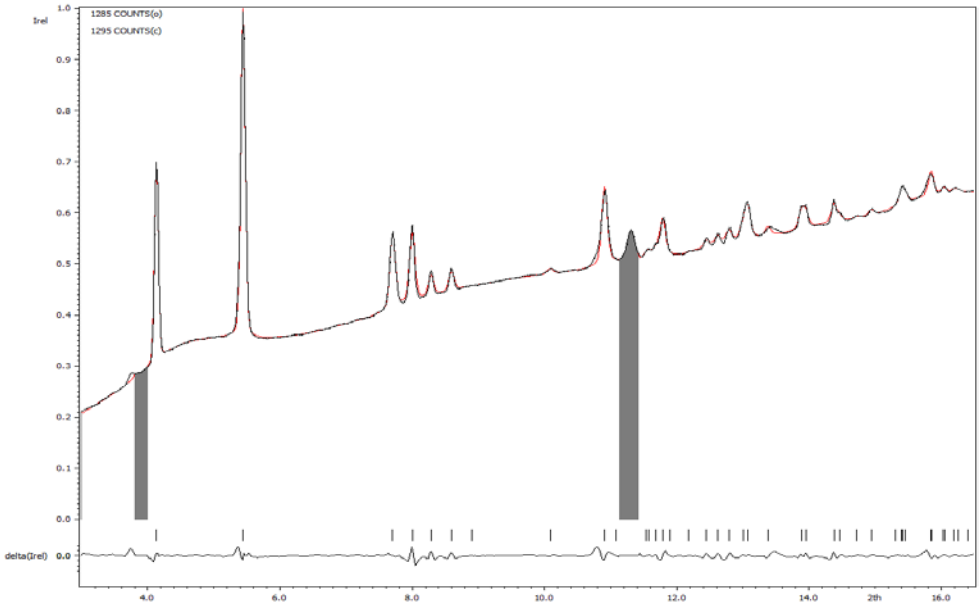

Figure S7. Structure-independent refinement of the unit-cell of the diffraction pattern obtained for the MIL-53(Cr)_Cl, space group *C2/c* : a=20.017(4) Å, b=7.883(8) Å, c=6.824(8) Å, β=106.67(2)° V=1031.5(4)Å^3 (Rp: 0.47, Rwp: 0.69, λ=0.69412 Å) at atmospheric pressure (first step of the experiment).

1.8. MIL-53(Cr)_CH_3

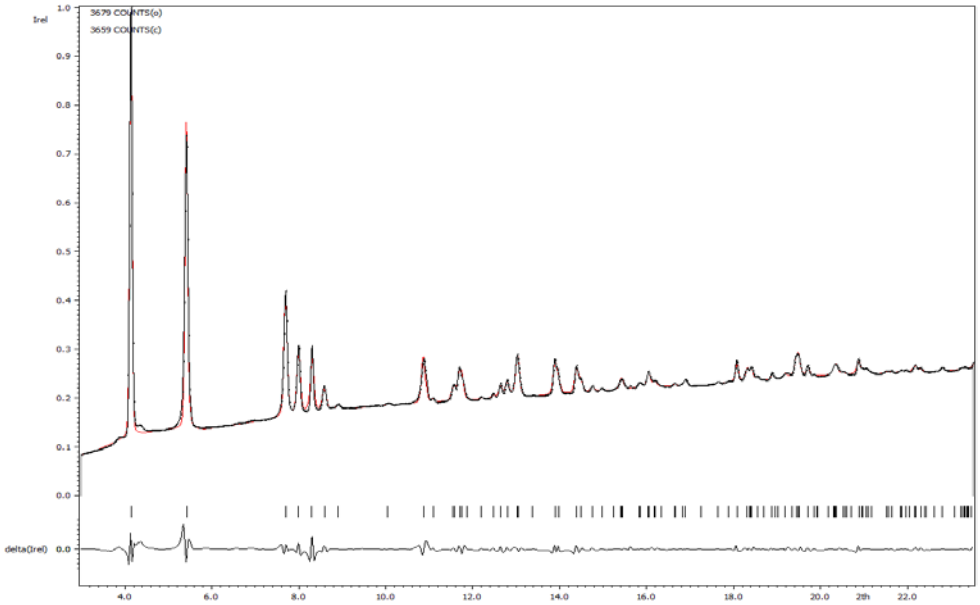

Figure S8. Structure-independent refinement of the unit-cell of the diffraction pattern obtained for the MIL-53(Cr)_CH_3, space group *C2/c* : a=20.062(2) Å, b=7.937(1) Å, c=6.820(1) Å, β=106.80(1)° V=1039.6(1)Å^3 (Rp: 1.12, Rwp: 1.57, λ=0.69412 Å) at atmospheric pressure (first step of the experiment).

1.9. MIL-53(Al) NO_2

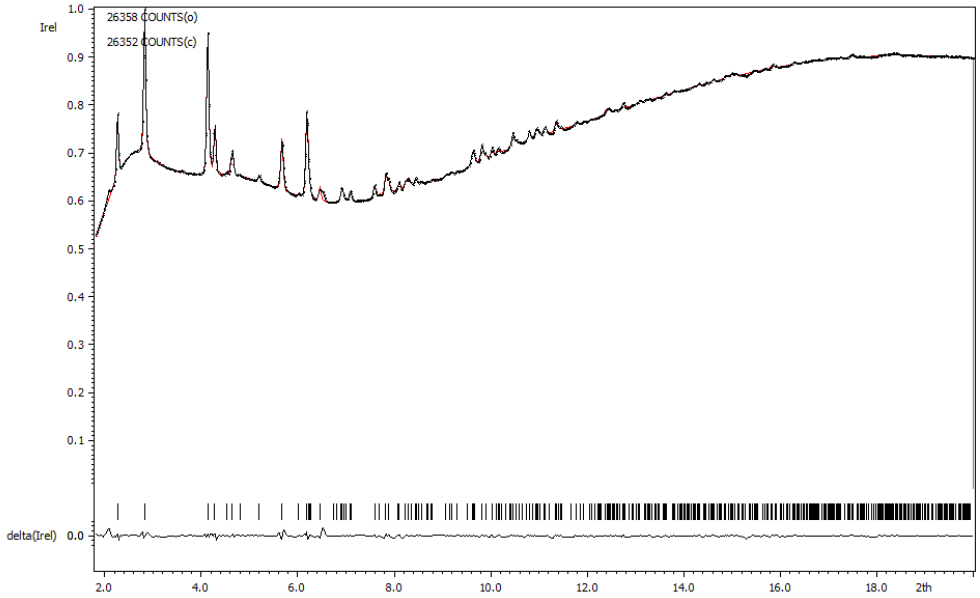

Figure S9. Structure-independent refinement of the unit-cell of the diffraction pattern obtained for the MIL-53(Al_NO_2, space group *C2/c* : a=19.743(3) Å, b=8.243(8) Å, c=6.647(7) Å, β=106.71(1)° V=1036.0(1) $Å^3$ (Rp: 0.18, Rwp: 0.31, λ=0.37380 Å) at atmospheric pressure (first step of the experiment).

1.10. MIL-53(Sc)

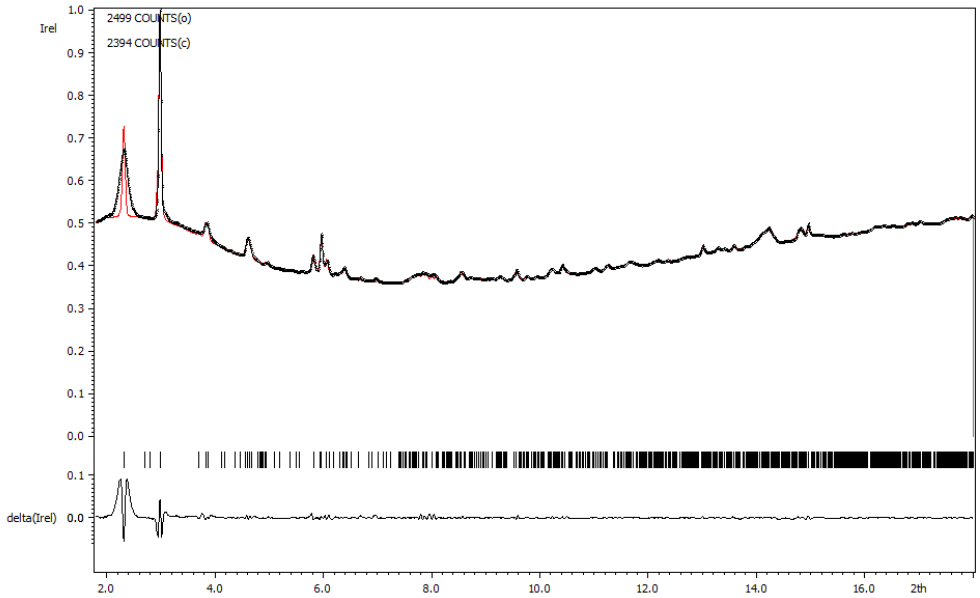

Figure S10. Structure-independent refinement of the unit-cell of the diffraction pattern obtained for the MIL-53(Sc), space group *P-1* : a=19.766(4) Å, b=7.609(2) Å, c=12.778(2) Å, α=88.27(2)°, β=92.05(2)°, γ=91.46(2)° V=1917.5(2)$Å^3$ (Rp: 0.60, Rwp: 0.92, λ=0.5100 Å) at atmospheric pressure (first step of the experiment).

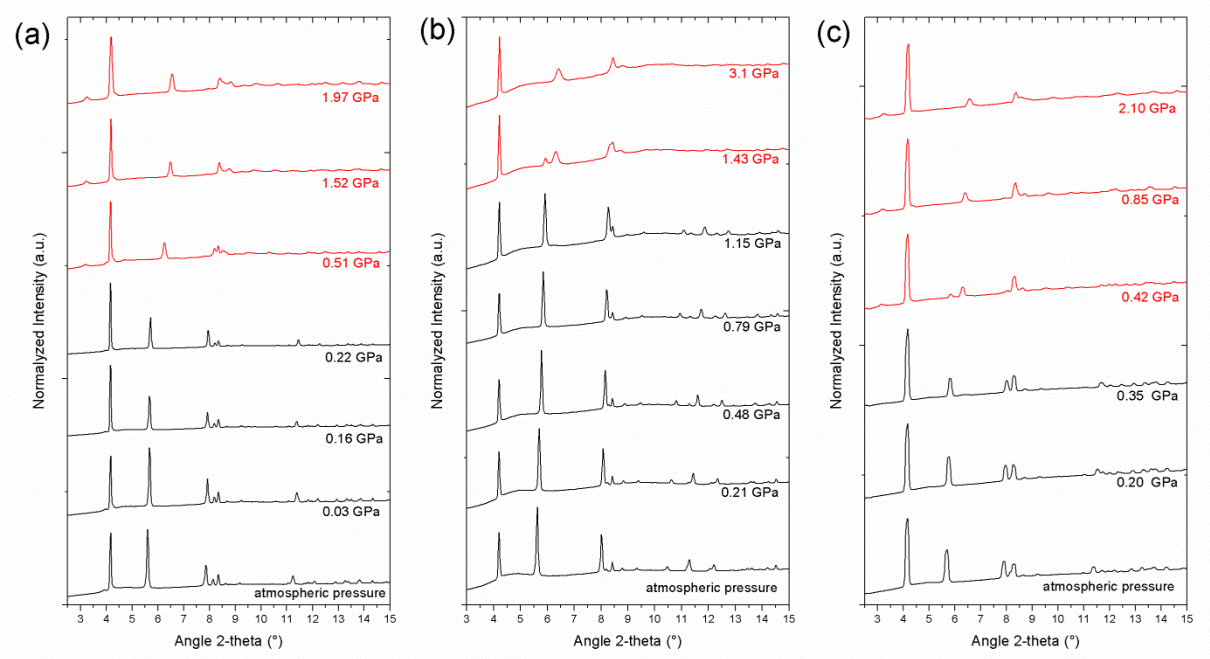

Figure S11. Powder X-ray patterns obtained for the (a) MIL-53(Cr), (b) MIL-53(Al) and (c) MIL-53(Fe) as a function of the applied pressure at room temperature. Patterns in black line correspond to the monoclinic (S.G. *C2/c*) hydrated Narrow Pore form and in red line to the triclinic (S.G. *P-1*) Very Narrow Pore form.

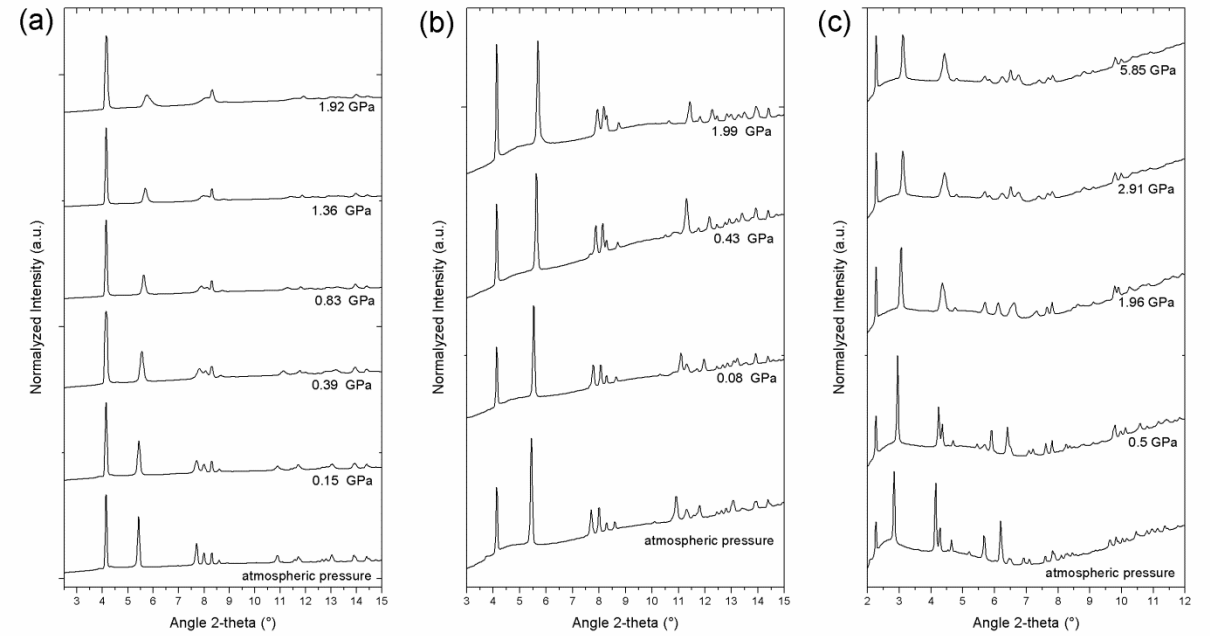

Figure S12. Powder X-ray patterns obtained for the (a) MIL-53(Cr)_Cl, (b) MIL-53(Cr)_CH_3 and (c) MIL-53(Al)_NO_2, as a function of the applied pressure at room temperature.

3. Bulk modulus determination

All the equations of state parameters where determined using EosFit7c software form R. J. Angel [5] using Murnaghan model [6].

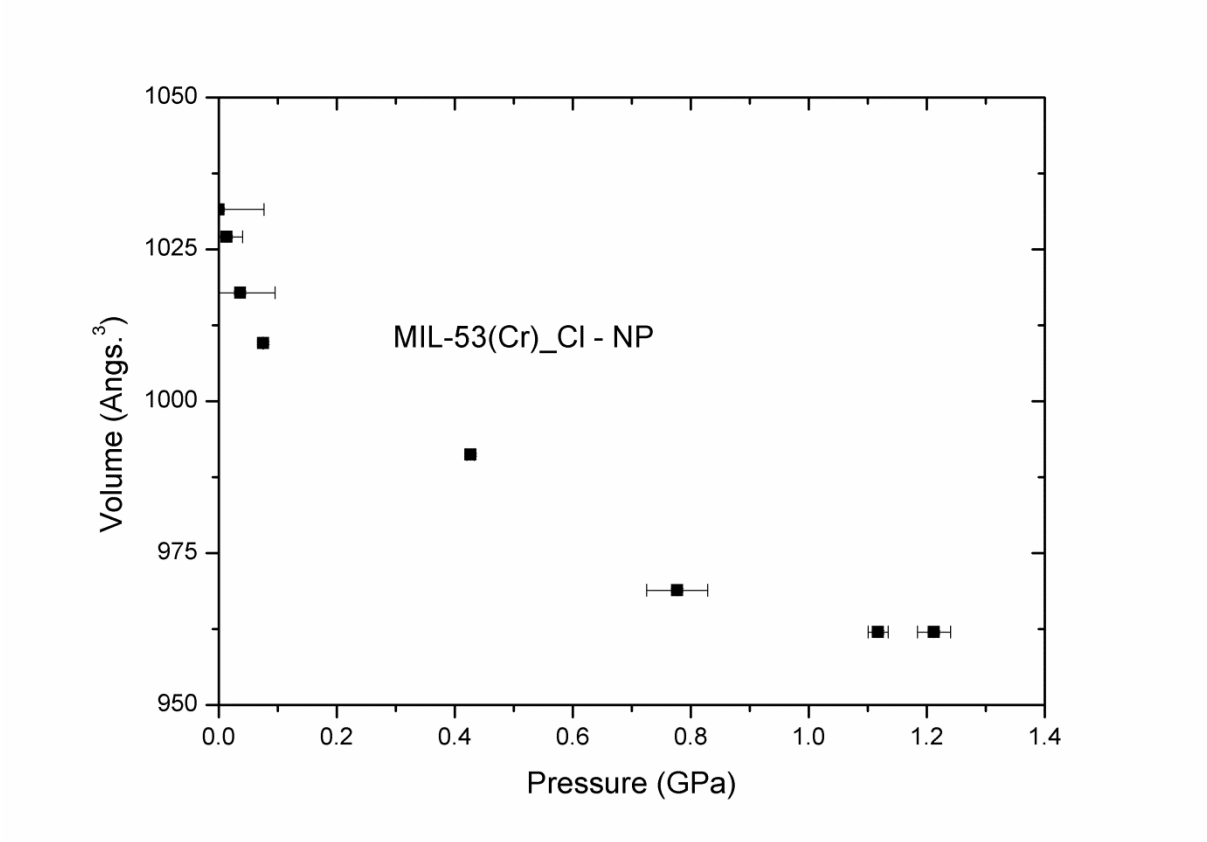

Figure S13. Evolution of the unit cell volume of the air-hydrated Narrow Pore form (S.G. *C2/c*) of MIL-53(Cr)_Cl.

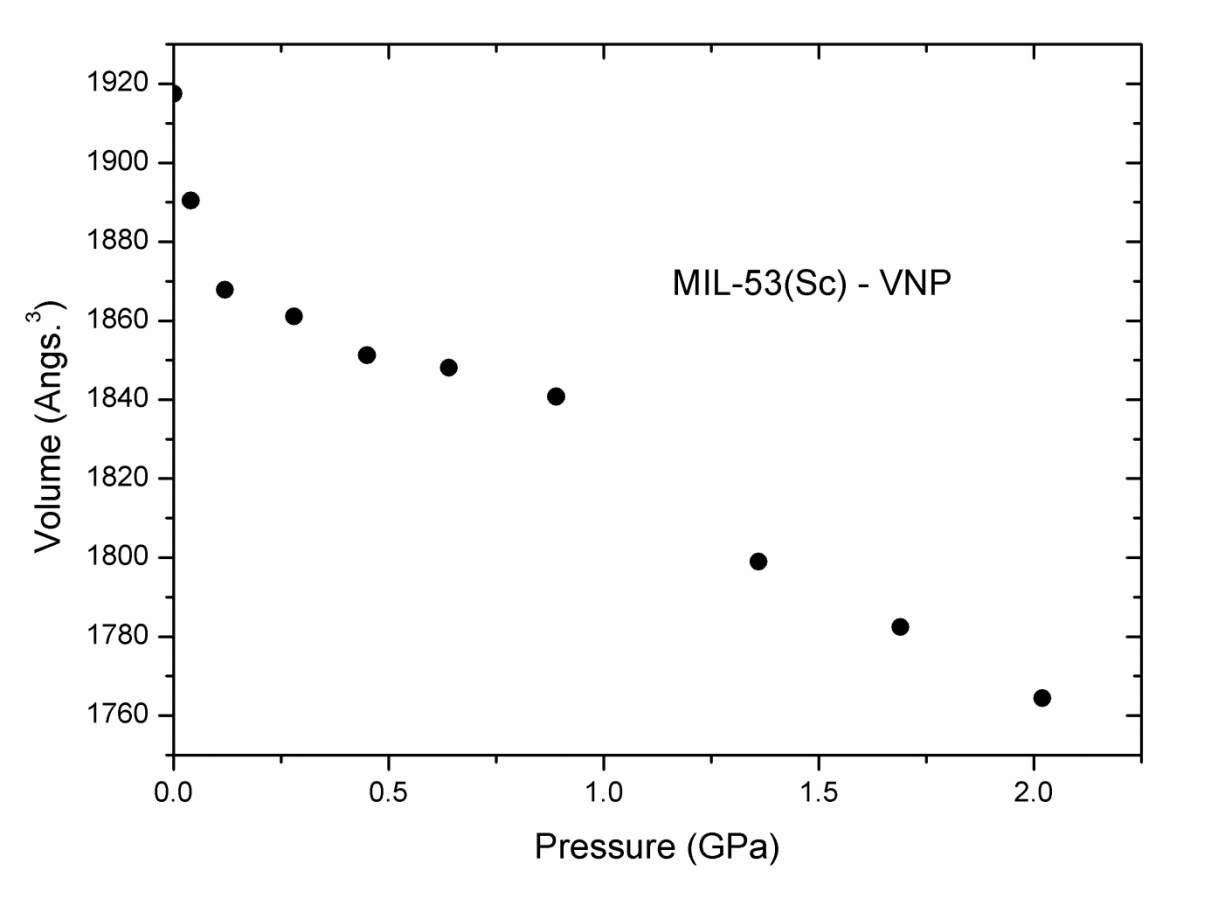

Figure S14. Evolution of the pressure-induced unit cell volume of the Very Narrow pore form of MIL-53(Sc).

Table S2. Equation of state parameters obtained using the Murnagham model for all the air hydrated MIL-53(M)_X forms with M=Al, Cr, Sc and X=NO_2, Cl, CH_3.

Compound	S.G.	V_0 (Å^3)	K_0 (GPa)	Kp	Density
MIL-53(Al)	*C2/c*	939.92(1)	10.7(1)	12.4(1)	1.47
MIL-53(Al)_NO_2	*C2/c*	1036.5(1)	7.3(1)	16.5(1)	1.52
MIL-53(Cr)	*C2/c*	987.2(1)	4.29(1)	2.1(1)	1.57
	P-1	909.2(1)	3.4(1)	9.6(1)	1.82
MIL-53(Cr)_Cl	*C2/c*	1016.7(1)	12.4(1)	18.6(1)	1.72
MIL-53(Cr)_CH_3	*C2/c*	1052.9(1)	3.7(1)	31.8(1)	1.58
MIL-53(Fe)	*C2/c*	986.1(1)	10.1(1)	1.5(1)	1.60
	P-1	946.8(1)	7.4(1)	106.7(1)	1.67
MIL-53(Sc)	*P-1*	1902.5(1)	10.3(1)	23.6(1)	1.57

The data reported in Table S2 shows that a correlation can be hardly found between the crystal density of the MIL-53s series and their bulk moduli since the variability of these solids in terms of density is too small to establish a reliable structure property relation.

References

[1] A. P. Hammersley, S. O. Svensson, M. Hanfland, A. N. Fitch, D. Häusermann, *High Press. Res.*, **1996**, 14, 235-248.

[2] H. K. Mao, J. Xu, P. M. Bell, *J. Geophys. Res.*, **1986**, 91, 4673-4676.

[3] A. Boultif, D. Louer, *J. Appl. Crystallogr.*, **1991**, 24, 987-993.

[4] V. Petricek, M. Dusek, L. Palatinus, *Z. Kristallogr.*, **2014**, 229, 345-352.

[5] R. J. Angel, M. Alvaro, J. Gonzalez-Platas, *Z. Kristallogr.*, **2014**, 229, 405-419.

[6] F.D. Murnaghan, *Proceedings of the National Academy of Sciences of the United States of America*, **1944**, 30, 244-247.